

11 **Current and future global climate impacts resulting from COVID-19**

12 Piers M. Forster* (1), Harriet I. Forster (2), Mat J. Evans (3,4), Matthew J. Gidden (5,12), Chris D.
13 Jones (6), Christoph A. Keller (7,8), Robin D. Lamboll (9), Corinne Le Quéré (10,11), Joeri Rogelj
14 (9,12), Deborah Rosen (1), Carl-Friedrich Schleussner (5,13), Thomas B. Richardson (1), Christopher
15 J. Smith (1,12), Steven T. Turnock (1,6)

16

- 17 1. Priestley International Centre for Climate, University of Leeds, UK (p.m.forster@leeds.ac.uk)
18 2. Queen Margaret's School, Escrick, York, UK
19 3. Wolfson Atmospheric Chemistry Laboratories, Department of Chemistry, University of York,
20 York, YO10 5DD, UK
21 4. National Centre for Atmospheric Science, University of York, York, YO10 5DD, UK
22 5. Climate Analytics, Berlin, Germany
23 6. Met Office Hadley Centre, Exeter, UK
24 7. NASA Global Modeling and Assimilation Office, Goddard Space Flight Center, Greenbelt,
25 MD, USA
26 8. Universities Space Research Association, Columbia, MD, USA
27 9. Grantham Institute for Climate Change and the Environment, Imperial College London, UK
28 10. School of Environmental Sciences, University of East Anglia, UK
29 11. Tyndall Centre for Climate Change Research, University of East Anglia, UK
30 12. Energy Program, International Institute for Applied Systems Analysis, Laxenburg, Austria
31 13. IRI THESys, Humboldt University, Berlin, Germany

32

33 **Abstract**

34 The global response to the COVID-19 pandemic has led to a sudden reduction of both greenhouse gas
35 emissions and air pollutants. Here using national mobility data we estimate global emission
36 reductions for 10 species over February-June 2020. We estimate global NO_x emissions declined by as
37 much as 30% in April, contributing a short-term cooling since the start of the year. This cooling trend
38 is offset by a ~20% reduction in global SO₂ emissions that weakens the aerosol cooling effect, causing
39 short-term warming. As a result, we estimate the direct effect of the pandemic driven response will be
40 negligible, with a cooling of around 0.01 ± 0.005 °C by 2030 compared to a baseline scenario which
41 follows current national policies. In contrast, with an economic recovery tilted towards green stimulus
42 and reductions in fossil fuel investments, it is possible to avoid a future warming of 0.3°C by 2050.

43
44 By the time the World Health Organization declared COVID-19 (scientifically referred to as the
45 severe acute respiratory syndrome–coronavirus 2 or SARS-CoV-2) a pandemic on 11 March 2020,
46 the virus had already spread from China, to other Asian countries, Europe and the US. As of 5 July
47 2020, cases have been identified in 188 countries or regions¹. This has led to unprecedented enforced
48 and voluntary restrictions on travel and work. This in turn has led to reductions of both greenhouse
49 gas emissions and air pollutants²⁻⁴. Analysis of Google⁵ and Apple⁶ mobility data shows mobility
50 declined by 10% or more during April 2020 in all but one of the 125 nations tracked. Mobility
51 declined by 80% in five or more nations (Figure S1). Associated declines in air pollution have been
52 observed from satellite data and from local ground based observations^{7,8}. The large pollution declines
53 are expected to be temporary as pollution levels are already returning to near normal levels in parts of
54 Asia^{9,10}.

55 Here we build an estimate of emission changes in greenhouse gases and air pollution due to the
56 COVID-19 global restrictions over February-June 2020 and project these into the future. These
57 emission changes are then used to make a prediction of the resultant global temperature response. We
58 examine the temperature response of a direct recovery to pre-COVID-19 national policies and

59 emission levels, and also explore responses where the economic recovery to COVID-19 is driven by
60 either a green stimulus package or an increase in fossil fuel use.

61 **Emission trends**

62 Bottom-up emission trend analyses have traditionally relied on a laborious collection of various
63 energy industry related indicators and statistics from multiple sources¹¹. The unprecedented recent
64 access to global mobility data from Google and Apple gives a unique opportunity to compare trends
65 across many countries with a consistent approach. We use this data to develop a new method of
66 emission trend analysis. The advantage over previous approaches is the possibility of near real time
67 analysis, national granularity and a systematic consistent approach across nations and over time. The
68 disadvantages are the loss of direct a connection between energy and emissions and the need to make
69 assumptions about these relationships. There are also disadvantages over the short time history of the
70 mobility data and opacity from the data providers around their detailed methodologies and
71 uncertainties. Here we make a simple set of assumptions to deduce emissions change estimates from
72 this mobility data and test the new emissions change estimates extensively against the approach of Le
73 Quéré et al.³.

74

75 Google and Apple mobility changes and the Le Quéré et al. data all indicate that over 50% of the
76 world's population reduced travel by over 50% during April 2020 (Figure 1a). Google mobility trends
77 indicate that over 80% of the population in the 114 countries in the dataset (4 billion people) reduced
78 their travel by more than 50%. Google mobility data and emission reduction estimates based on
79 confinement level analysis in Le Quéré et al. agree on country level surface transport trends to within
80 ~20% (Figures 1b and S1). When we examine the trends for the countries that we expect have
81 contributed most to the overall surface transport emission change (e.g. USA, European nations and
82 India), good agreement between the datasets is observed, and their trends are well correlated in time
83 (see Figure 1b and Figure ED1). Workplace, retail and residential movement data from Google also
84 compare relatively well with corresponding industry, public and residential sector emission changes

85 but only if the high estimate of the emission change in the Le Quéré et al. dataset (Figures 1b, 1c and
86 S3 and S4) is employed.

87

88 Employing mobility data outside of the surface transport sector is likely to overestimate the emission
89 change and this appears to be the case for CO₂ emissions when compared to two previous estimates^{1,2}.

90 Nevertheless, our national and US state level mobility-derived emission estimates are well correlated
91 in time with emission changes from the Le Quéré et al. study (see examples in Figures S3 and S4).

92 For the industry sector, differences may be due to the fact that the emissions from industrial activity
93 are less correlated with mobility trends, due to automated machinery, inertia in closing operations, or

94 alternative modes of work or a base-line level of industrial emission from heavy industry in the
95 absence of production, neither which would be captured by the Google mobility data which only

96 reports changes in phone locations. For the residential sector, the 20% median increase matches the
97 UK smart meter analysis by Octopus Energy for the situation when previously empty houses were

98 occupied during the day after lockdown restrictions began¹². However, many households were already
99 occupied during the day and in these situations when an additional occupant was added, energy use

100 only increased by 4%. These factors likely mean that our Google-based trends overestimate the
101 emission change from these sectors, leading to our Google based total emission trend estimate

102 agreeing better with the high emission estimate from the Le Quéré et al. dataset. Our analysis also
103 suggests considerably larger trends than found in Liu et al.² (compare datasets in Figure 1c). There is

104 also a question about how representative the Apple and Google datasets are of wider national
105 behaviour and how the use and penetration of these phone operating systems varies across regions¹³.

106 For example, the over 80% drop in Apple driving mobility in India (Figure 1a and S1), may only
107 represent the part of the population that are able to work from home. Therefore, the emissions trends

108 in our work which are largely derived from Google mobility data should be taken as a high estimate
109 of the COVID-19 emission driven change (see methods section a).

110

111 In the following we construct 2020 emission changes largely from Google mobility data to estimate
112 emissions changes from the restriction measures in response to the COVID-19 virus, as illustrated in

113 Figure 1c. As Google data is not available everywhere, we employ the Le Quéré et al. analysis to
114 cover important missing countries, in particular, China, Russia and Iran which are all large emitters
115 whose citizens have been under significant restrictions related to COVID-19. We also use Le Quéré et
116 al. data to provide additional trend estimates from aviation and shipping sectors (see methods section
117 a).

118

119 **Figure 1.** Comparison of sector emission trends. a) Population weighted histogram of surface
120 transport trends from Apple driving data, Google transit mobility data and the high estimate from Le
121 Quéré et al. for available countries in the different datasets averaged over April 2020. b) Violin plots
122 showing the distribution, minimum, maximum and median levels of national trends weighted by CO₂
123 emissions for the Google and Le Quéré datasets and the differences between the datasets evaluated
124 over April 2020. c) Estimates of emission changes for the datasets across four sectors for April 2020
125 and the sum of the four sectors. The CO₂ emission estimates from Liu et al.² are also shown on this
126 panel. In Figures 1b and 1c data is shown for 60 countries with overlapping data in the Google and Le
127 Quéré datasets (representing 60% of global CO₂ emissions). In Figure 1c, Apple data are for 57
128 countries, covering 58% of the global emissions. The Liu et al.² estimate is for a global emission
129 change. The high estimate from Le Quéré et al. data is used in Figures 1a and 1b. Figure 1c shows the
130 Le Quéré et al. low and high estimates as the range of the error bar on the mid-level estimate. For
131 baselines, see methods section a.

132

133 Our bottom up analysis uses 123 countries covering over 99% of global fossil fuel CO₂ emissions,
134 extending the 69 countries analysed in Le Quéré et al. Daily national emission trends in six sectors are
135 analysed for January-June 2020 (surface transport, residential, power, industry, public, and aviation).
136 These are then weighted by the national and sector split of seven emitted species covering the major
137 greenhouse gases and short-lived pollutants. The estimated changes in these non-CO₂ species covers
138 their total anthropogenic emissions, although agricultural and waste emissions are assumed not to
139 change (methods section b). National and sector data are taken from the Emissions Database for

140 Global Atmospheric Research (EDGAR) version 5.0 database for 2015¹⁴. These data are combined to
141 generate national and globally averaged daily emission changes in 2020 by species and sector.

142

143 In order to assess changes due to the COVID-19 pandemic, we establish a baseline scenario. We take
144 a central estimate of emissions pathways¹⁵, in which countries are assumed to meet their stated
145 Nationally Determined Contributions (NDCs) by 2030. In this baseline, no further strengthening of
146 climate action after 2030 is assumed to take place. These pathways account for both greenhouse gas
147 and air pollutant emission changes (see methods section c). To derive changes from this scenario a
148 three-stage process is followed (see methods section a). First, fractional Google mobility data
149 employs the 5-week period (Jan 3–Feb 6, 2020) as reference. Absolute emission trends are then
150 computed by multiplying these fractional changes by either the 2019 CO₂ emissions from Le Quéré et
151 al. or, for other species, the 2015 emissions in the EDGAR database¹⁴. Finally these absolute changes
152 are then applied to a steadily rising emission pathway based on pre-COVID-19 national pledges (see
153 Table 1). Only the globally average emission changes are used in this paper (see Figure 2a), but
154 national and spatially gridded data are made available for other interested researchers¹⁶.

155

156 Our analysis shows that emission reductions likely peaked in mid-April 2020 and that these
157 reductions are species dependent. The data suggests that global fossil fuel CO₂ emissions and total
158 NO_x emissions could have decreased by as much as 30% in April 2020 driven by a decline in surface
159 transport emissions (Figures 2a, 2b and S5). Conversely, organic carbon (OC) has increased by <1%
160 as it is primarily affected by rising residential emissions (Figures 2b and S5). Methane changes are
161 driven by power sector declines, and SO₂ is most strongly affected by declining industrial emissions.
162 Generally, changes in surface transport are the biggest driver of change for most species analysed
163 (Figure S5). The analysis in Figure 2b also applies our methods to the Le Quéré et al. data for non-
164 CO₂ species and reports both previous estimates of CO₂ trend. Our estimated trends are close to the
165 high Le Quéré et al. estimate, and almost twice as large as the CO₂ trend estimate of Liu et al.².

166

167 **Figure 2.** Species derived changes from COVID-19 restrictions. a) Percentage globally averaged
168 emission changes for the considered species as a function of day in the year of 2020. The changes are
169 for fossil fuel CO₂ emissions and total anthropogenic emissions from the other sectors. b) A
170 breakdown of the April 2020 average global emission reductions compared to a recent year for the
171 different species. The breakdown is for major emission-nations, including international aviation.
172 Global percentage emission changes from the baseline are shown on the x-axis (see details in Figure
173 S6). Trends are relative to 2019 for CO₂, for the other species they are relative to 2015. The low, mid
174 and high estimates of the total changes based on Le Quéré et al.³ and Liu et al.² trends are shown for
175 comparison as the black circles, error bars and red triangle.

176

177 Our data suggests that changes in emissions are not confined to the major emitting countries, and
178 mobility restrictions have been of worldwide proportions (despite the extent of measures – and
179 therefore relative emissions changes – varying globally) during April 2020 (Figure 1 and S1). This
180 manifests itself in many countries contributing to the emission decline. For the short-lived species,
181 Europe and the United States, in spite of their large fractional national emission change, make up a
182 small percentage of the global response due their relatively low levels of emissions from pollution
183 (Figure 2b and S6).

184

185 **Observational evidence**

186 Detecting a COVID-19 related signal in CO₂ concentrations is challenging due to CO₂'s long
187 atmospheric lifetime which makes any perturbation small. While the airborne fraction of CO₂
188 emissions is approximately 50% on multi-annual timescales¹¹, the airborne fraction of emissions
189 changes is likely above 90% on sub-annual timescales¹⁷. Because CO₂ is not well mixed on the
190 timescale of weeks to months, individual observing stations will not reflect the global CO₂ burden –
191 for example Mauna Loa in the Northern hemisphere Pacific Ocean may see a larger signal than at the
192 South Pole from the emissions reductions due to COVID-19 restrictions. The magnitude of natural –
193 terrestrial and marine – fluxes of CO₂ compared with anthropogenic emissions make it extremely
194 difficult to detect changes in emissions at national level from CO₂ concentrations themselves. We

195 estimate these CO₂ concentration changes in the temperature response to restrictions section (see
196 Figure ED2 and 5b) and find maximum reductions compared to our baseline scenario of around 2
197 ppm in two years' time (Figure ED2).

198

199 Even though the CO₂ change cannot readily be observed, changes in the concentrations of air
200 pollutants can be employed to test the veracity of the bottom-up emission reduction estimates. A
201 decline in NO₂ has been observed globally, and in several countries and cities^{7,8}. NO₂ is short-lived
202 (~5 hours), provides a relatively linear response to emission changes (unlike other pollutants such as
203 O₃ and PM_{2.5}), and reductions in its emissions are expected to be well correlated to CO₂ emission
204 reductions (Figure 2a, Le Quéré et al.). Changes in its concentration thus act as a useful bellwether
205 for changes in CO₂ emissions. A number of studies report COVID-19 induced changes in NO₂
206 concentration from both surface and satellite platforms over China^{18,19}. However, it remains
207 challenging to get a quantifiable estimate of the emission-driven NO₂ change as it is hard to separate
208 that signal from meteorological variability. To address this we follow previous work²⁰ and develop a
209 machine learning method to derive meteorology and chemistry-normalized changes in NO₂ surface
210 concentrations at air quality monitoring stations around the globe (see methods section d). We
211 aggregate these changes for 32 nations and show how these observationally-based national time-series
212 of NO₂ concentration changes compare to our mobility-based estimate of NO_x emissions change in
213 Figure S7. Figure 3 shows the average observationally-derived NO₂ change versus the predicted
214 mobility-based NO_x emissions change for each country in 2020. Some differences between the
215 emission estimates and observed changes would be expected: monitoring stations tend to focus on
216 sites with high surface transport emission and so may be less sensitive to changes in industrial or
217 residential activity; much of the surface transport emissions of NO_x arises from commercial vehicles
218 (64% of surface transport emission in the UK²¹) which may show different responses to the
219 population aggregated mobility data used here (see methods section a and Figure S2). However, the
220 comparisons for the individual countries (Figure S7) are generally good and there is a quantitative
221 relationship between the average predicted change in the emissions and observed reduction in
222 concentrations (Figure 3). Most countries show a smaller (20% or roughly 2 percentage points)

223 decrease in observed NO₂ than the predicted reduction in NO_x emissions, whereas China and India
224 show larger observed reductions than predicted (28% and 48% respectively). This could be due to the
225 Le Quéré et al. analysis being used to estimate trends in China as Google data was not available and
226 also due a possible lack of representativeness in the phone mobility data for India (see the emission
227 trends section). As China is the largest emitter this might that our analyses might be affected by a
228 possible significant underestimate of Chinese NO_x trends and hence global trend in the early part of
229 the record, although any global underestimate is unlikely to have persisted into April, where the
230 contribution of China to the global trend is relatively modest (Figure 2b).

231

232 **Figure 3.** Comparison of predicted NO_x emission change with NO₂ observations. Country level
233 comparison of the mean predicted NO_x emissions change against the meteorologically-normalized
234 observed mean fractional reduction in NO₂ concentration for the period 1/1/2020 to 11/5/2020. Circle
235 size indicates the mass of NO_x emitted each day for that country from EDGAR emissions. Blue line
236 shows the line of best fit (orthogonal regression) excluding China and India shown in red, weighted
237 by the number of observations in those countries, with the shaded area showing the 95% confidence
238 interval. Not all countries are labelled. Brazil shows an increase in NO₂ concentrations and is not
239 shown but is included in the statistical fit (see Figure S7).

240 **The temperature response to restrictions**

241 The immediate response of the warming comes from a combination of an aerosol induced warming
242 trend and a cooling trend both from CO₂ reductions and the NO_x-driven tropospheric ozone cooling
243 loss (Figure 4). To estimate the surface temperature response beyond April 2020, the emission trends
244 are projected forward in time under four simple “what-if” assumptions. The temperature changes
245 from these pathways were simulated by the FaIRv1.5 climate emulator²² which was set up to
246 represent the response expected from the latest generation of climate models (see methods section e).
247 As significant social distancing conditions may be necessary for two years²³, we begin by assuming in
248 all pathways that the emissions decrease will remain at 66% of their June 2020 values until the end of

249 2021. In the simplest “two-year blip” pathway emissions return linearly to the baseline pathway by
250 the end of 2022 (Table 1, Figure 4a). Under such a pathway, we project a longer-term cooling from
251 reductions in CO₂ of around 0.01 ± 0.005 °C compared to baseline, with a cancellation of the
252 influence of the removal of short-term pollutants (Figures 4b and ED2).

253

254 As the global temperature response due to COVID-19 restrictions will likely be small, climate
255 scientists are encouraged to look for regional climate signatures. In particular changes in aerosol
256 loadings may contribute to increasing regional risks posed by extreme weather such as heat waves or
257 heavy precipitation^{24,25}. Such near-term changes require particular attention as hazards posed by
258 extreme weather will compound with the ongoing pandemic situation, as exemplified tragically by
259 tropical cyclone Amphan hitting Kolkata on 21 May 2020. With considerable overlaps of vulnerable
260 groups (for example heat waves and the elderly) or challenges related to the implementation of
261 effective responses (evacuation in case of flooding), as well as potential impacts on crop yields²⁶ and
262 initial studies suggesting that the spread of COVID-19 may itself be influenced by climatic factors²³,
263 this will put the ability of society and governments to manage compound risks to the test²⁷.

264

265 In our estimates, declines in NO_x of as much as 30% contribute a short-term cooling of up to 0.01 °C
266 over 2020-2025 almost exclusively from reductions in tropospheric ozone. NO_x trends also contribute
267 an insignificant warming effect from the decrease in nitrate aerosol. As the ozone response is
268 expected to have strong regional variation, we test the ozone response in a more sophisticated
269 emulator^{28,29} that takes these variations into account (see methods section f). This estimates an annual
270 mean radiative forcing of -0.029 Wm^{-2} for 2020, in very close agreement with the forcing seen in
271 Figure 4a (-0.030 Wm^{-2}). The emulator also provides an estimate of the regional mean surface ozone
272 changes (Table S4). In contrast to NO_x, reductions in emissions of other short-lived pollutants,
273 especially SO₂, cause a warming from a weakening negative aerosol forcing. These two effects more
274 or less cancel in our simulations, although on balance we expect a small warming effect over the next
275 5 years (Figure 4).

276

277 In spite of the uncertainty, our results indicate that reductions of NO_x have a cooling effect which will
 278 likely offset a considerable fraction of the warming that comes from reductions in emissions of other
 279 short-lived pollutants. This suggests that policies directed at limiting pollution from road transport
 280 could offset the short-term warming that might come from policies that reduce pollution from the
 281 power and industry sector. Therefore, we recommend policies are enacted to cut pollution from all
 282 three sectors at the same time. This is a useful way forward for net-zero transition pathways so we can
 283 avoid any short-term warming effects that might come from reductions in aerosol pollution³⁰.

284 **The need for a green recovery**

285 As we have shown, the climate effect of the immediate COVID-19 related restrictions is close to
 286 negligible and lasting effects, if any, will thus only arise from the recovery strategy adopted in the
 287 medium-term. To that end, we assess the effect of different scenarios including a fossil-fuel recovery,
 288 and two different scenarios of green stimulus (all pathway assumptions are summarised in Table 1).
 289

290 **Figure 4.** Effective radiative forcing and temperature response. Results are for the two-year blip
 291 pathway compared to the baseline pathway. The response is broken down by the major forcing
 292 contributors, as emulated by the FaIRv1.5 model. 5%–95% Monte-Carlo sampled uncertainties are
 293 shown and weighted according to their historical fit to the surface temperature record (see methods
 294 section e).

295

296 *Table 1, Pathway what-if assumptions*

Pathway	What happens	Notes
Baseline	Follows emissions until 2030 consistent with a successful implementation of the current Nationally Determined Contributions (NDC) submitted by individual countries under the Paris Agreement, adapted from Rogelj et al (2017) ¹⁵ . Emissions continue after 2030 assuming no significant strengthening in climate action.	The data is adapted from Rogelj et al. (2017) ¹⁵ and represents a central estimate of the range of estimates presented therein. This pathway also falls centrally in

		the range identified by the 2019 UNEP Emissions Gap Report ³¹
Two-year blip	Reflecting potential SARS-CoV-2 transmission dynamics ²³ this case explores 66% of the June 2020 lockdown persisting until the end of 2021, then emissions linearly recover to baseline by the end of 2022.	This implies a persistent necessity of partial lockdowns until the end of 2023, but with no lasting effect of SARS-CoV-2.
Fossil-fuelled recovery	Follows the two-year blip pathway until end of 2021, then emissions recover in a way similar to the recovery after the 2008/9 global recession, rebounding to 4.5% above the baseline at the end of 2022. Stimulus packages are designed with strong support for fossil-fuel energy supply, resulting in more fossil investment than a pre-COVID-19 current policy scenario (+1%) and considerably less in low-carbon alternatives (-0.8%). Resulting emissions are 10% higher in 2030 than the baseline scenario, a trend which is assumed to continue thereafter ³² .	2030 data taken from Climate Action Tracker ³² , “rebound to fossil fuel scenario” with the relative increase in emissions compared to baseline continued thereafter.
Moderate Green stimulus	Follows the two-year blip pathway until end of 2021, then emissions recover slightly, until the end of 2022, but never reach the baseline projections. Governments choose recovery packages to target specifically low-carbon energy supply and energy efficiency, and do not support bailouts for fossil firms. The resulting investment differential (+0.8% for low-carbon technologies and -0.3% for fossil fuels relative to a current-policy scenario) begins to structurally change the emissions intensity of economic activity, resulting in about a 35% decrease in greenhouse gas emissions by 2030 relative to the baseline scenario, a trend which is assumed to continue thereafter ³² , consistent with meeting global net-zero CO ₂ by 2060.	Short-term benefits come from changes to the norms of behaviour, then green incentives to decarbonize all sectors of the economy
Strong green stimulus	As the moderate green stimulus with investment differentials (+1.2% for low-carbon technologies and -0.4% for fossil fuels relative to a current policy scenario), resulting in a slightly more than 50% decrease of greenhouse gas emissions by 2030 relative to the baseline scenario. This trend is continued thereafter, consistent with meeting global net-zero CO ₂ by 2050.	This has over 50% chance of limiting the 2050 temperature rise to 1.5 °C above preindustrial

298 Due to the different warming and cooling trends from short-lived pollutants, the 2020-2030 climate
299 response to the different pathways remains uncertain but is likely negligible whatever path the
300 recovery takes (Figures 4, 5, ED3 and ED4). However, differences manifest themselves after 2030.
301 Figure 5 shows estimated changes in CO₂ emissions and the climatic responses for the four assessed
302 pathways. We find that both the two-year blip pathway, where the economic recovery maintains
303 current investment levels, or the fossil fuelled recovery pathway, are likely to exceed a 2°C above
304 preindustrial limit by 2050 (>80%, Figure ED5). Conversely, choosing a pathway with strong green
305 stimulus assumptions (~1.2% of global GDP), including climate policy measures, has a good chance
306 (~55%, Figure ED5) to keep global temperatures change above preindustrial within the 1.5 °C limit
307 saving around 0.3 °C of future warming by 2050 (0.2°C for the moderate green stimulus pathway).

308
309
310
311
312
313
314
315
316

317 **Figure 5.** Longer term climate response. a) Emissions of CO₂, b) CO₂ concentrations, c) the surface
318 air temperature response for the what-if pathways from Table 1, emulated by the FaIRv1.5 model.
319 The baseline pathway is also plotted, but largely obscured by the two-year-blip pathway. 5%–95%
320 Monte-Carlo sampled uncertainties are shown and weighted according to their historical fit to
321 observations³³ shown in panel c (see methods section e).

322
323
324
325

Our work shows that the global temperature signal due to the short-term dynamics of the pandemic is likely to be small. These results highlight that without underlying long-term system-wide decarbonisation of economies, even massive shifts in behaviour, only lead to modest reductions in the

326 rate of warming. However, economic investment choices for the recovery will strongly affect the
327 warming trajectory by mid-century. Pursuing a green stimulus recovery out of the post-COVID-19
328 economic crisis can set the world on track for keeping the long-term temperature goal of the Paris
329 Agreement within sight.

330

331 Lastly, by combining large datasets from surface air quality networks with mobility data, we have
332 illustrated the science benefits from timely and easy access to big data. Such data syntheses can help
333 epidemiology and environmental sciences provide the evidence base for the solutions that are urgently
334 needed to build a resilient recovery to the devastating pandemic. Google, Apple and other big data
335 providers are encouraged to continue to provide and expand their data offerings.

336

337

338 **References**

- 339 1. COVID-19 Map - Johns Hopkins Coronavirus Resource Center. Available at:
340 <https://coronavirus.jhu.edu/map.html>. (Accessed: 5 July 2020)
- 341 2. Liu, Z. *et al.* COVID-19 causes record decline in global CO₂ emissions. Preprint at
342 <http://arxiv.org/abs/2004.13614> (2020).
- 343 3. Le Quéré, C. *et al.* Temporary reduction in daily global CO₂ emissions during the COVID-19 forced
344 confinement. *Nat. Clim. Chang.* *10*, 647–653 (2020).
- 345 4. COVID-19 Air Quality Worldwide dataset. Available at: <https://aqicn.org/data-platform/covid19/>.
346 (Accessed: 5th July 2020)
- 347 5. Google LLC Community Mobility Reports. Available at: <https://www.google.com/covid19/mobility/>.
348 (Accessed: 5 July 2020)
- 349 6. Apple LLC Mobility Trends Reports. Available at: <https://www.apple.com/covid19/mobility>.
350 (Accessed: 5 July 2020)
- 351 7. Bauwens, M. *et al.* Impact of coronavirus outbreak on NO₂ pollution assessed using TROPOMI and
352 OMI observations. *Geophys. Res. Lett.* *47*, e2020GL087978 (2020).
- 353 8. Shi, X. & Brasseur, G. P. The response in air quality to the reduction of Chinese economic activities
354 during the COVID-19 outbreak. *Geophys. Res. Lett.* *47*, e2020GL088070 (2020).

- 355 9. China's air pollution overshoots pre-crisis levels for the first time. Available at:
356 <https://energyandcleanair.org/china-air-pollution-rebound-briefing/>. (Accessed: 24th May 2020)
- 357 10. Zhang, R. *et al.* NOx emission reduction and recovery during COVID-19 in East China. *Atmosphere*
358 *(Basel)* **11**, 433 (2020).
- 359 11. Friedlingstein, P. *et al.* Global carbon budget 2019. *Earth Syst. Sci. Data* **11**, 1783–1838 (2019).
- 360 12. Domestic energy usage patterns during social distancing | Octopus Energy. Available at:
361 <https://octopus.energy/blog/domestic-energy-usage-patterns-during-social-distancing/>. (Accessed: 24th
362 May 2020)
- 363 13. Operating System Market Share Worldwide | StatCounter Global Stats. Available at:
364 <https://gs.statcounter.com/os-market-share#quarterly-201903-201903-map>. (Accessed: 24th May 2020)
- 365 14. Crippa, M. *et al.* High resolution temporal profiles in the Emissions Database for Global Atmospheric
366 Research. *Sci. Data* **7**, 1–17 (2020).
- 367 15. Rogelj, J. *et al.* Understanding the origin of Paris Agreement emission uncertainties. *Nat. Commun.* **8**,
368 1–12 (2017).
- 369 16. Sector and gridded data available at DOI 10.5281/zenodo.3957826.
- 370 17. Jones, C. D. *et al.* Simulating the Earth system response to negative emissions. *Environ. Res. Lett.* **11**,
371 95012 (2016).
- 372 18. Le T. *et al.*, Unexpected air pollution with marked emission reductions during the COVID-19 outbreak in
373 China, *Science* (2020)
- 374 19. Liu F. *et al.*, Abrupt decline in tropospheric nitrogen dioxide over China after the outbreak of COVID-
375 19, *Science Advances* (2020).
- 376 20. Grange, S. K. and D. C. Carslaw. Using meteorological normalisation to detect interventions in air
377 quality time series, *Science of The Total Environment*, 653, 578–588 (2019).
- 378 21. Richmond B *et al.* *UK Informative Inventory Report (1990 to 2018)* (BEIS, London, 2020).
- 379 22. Smith, C. J. *et al.* FAIR v1.3: A simple emissions-based impulse response and carbon cycle model.
380 *Geosci. Model Dev.* **11**, 2273–2297 (2018).
- 381 23. Kissler, S. M., Tedijanto, C., Goldstein, E., Grad, Y. H. & Lipsitch, M. Projecting the transmission
382 dynamics of SARS-CoV-2 through the postpandemic period. *Science* **368**, 860-868 (2020).
- 383 24. Luo, F. *et al.* Projected near-term changes of temperature extremes in Europe and China under different

- 384 aerosol emissions. *Environ. Res. Lett.* **15**, 034013 (2020).
- 385 25. Samset, B. H. *et al.* Climate impacts from a removal of anthropogenic aerosol emissions. *Geophys. Res.*
386 *Lett.* **45**, 1020-1029 (2018).
- 387 26. Dentener, F. *et al.* Lower air pollution during COVID-19 lock-down: improving models and methods
388 estimating ozone impacts on crops. Preprint at: <https://eartharxiv.org/de9fs/>.
- 389 27. Phillips, C. A. *et al.* Compound climate risks in the COVID-19 pandemic. *Nat. Clim. Chang.* **10**, 586-
390 588 (2020).
- 391 28. Turnock, S. T. *et al.* The impact of future emission policies on tropospheric ozone using a parameterised
392 approach. *Atmos. Chem. Phys.* **18**, 8953–8978 (2018).
- 393 29. Turnock, S. T., Wild, O., Sellar, A. & O'Connor, F. M. 300 years of tropospheric ozone changes using
394 CMIP6 scenarios with a parameterised approach. *Atmos. Environ.* **213**, 686–698 (2019).
- 395 30. Shindell, D. & Smith, C. J. Climate and air-quality benefits of a realistic phase-out of fossil fuels.
396 *Nature* **573**, 408–411 (2019).
- 397 31. United Nations Environment Programme. *Emissions Gap Report 2019* (UNEP, Nairobi, 2020).
- 398 32. Climate Analytics/New Climate Institute. *Climate Action Tracker update: A Government Roadmap for*
399 *Addressing the Climate and Post COVID-19 Economic Crises Summary and Conclusions (Climate*
400 *Action Tracker, 2020)*.
- 401 33. Cowtan, K. & Way, R. G. Coverage bias in the HadCRUT4 temperature series and its impact on recent
402 temperature trends. *Q. J. R. Meteorol. Soc.* **140**, 1935–1944 (2014).

403

404 **Methods**

405 a) CO₂ emission estimates

406 *The Google Mobility analysis.*

407 Google⁵ and Apple⁶ mobility data were accessed on 5 July 2020. National average Google data was
408 used for 114 countries, and the US states. Mobility was provided in 6 categories of which we used
409 four in our analyses (transit stations, residential, work places, retail and recreation). These data
410 represent the number of Android phones at assigned locations, representing transit stations, homes,
411 work-places, retail outlets and parks. Apple mobility data was from phone movement changes

412 available for 57 countries providing data on changes in transit use, walking and driving, depending on
413 country. Google data was referenced to the day of the week average in the 5-week period Jan 3–Feb 6,
414 2020. Apple employed a baseline of 13 February and did not account for day of week effects. The
415 Apple data was considerably more variable and was only used as a check on the other datasets. Our
416 tests found that the Google transit mobility trends agreed well with Apple driving trends in the 56
417 nations with overlapping data (Figures 1a, S1 and ED1) and this gave us confidence to employ the
418 Google mobility data as an estimate of general trends in emissions from surface transport.
419 Correlations of the Apple driving data with Google transit data were stronger than 0.8 (over February-
420 June 2020) for 37 countries and their trends typically agreed to within 20% for April 2020 (Figure
421 ED1). For the UK Apple driving data agrees well with government analysis of car journeys (Figure
422 S2), whereas Google transit data appears to be more of a hybrid measure. Note, as discussed in the
423 observational evidence section, NO_x emissions might be expected to be more closely aligned to
424 commercial vehicles, and changes for these vehicles in the UK over the period of COVID-19
425 restrictions were less than indicated by either Apple or Google data (compare light van and heavy
426 goods vehicle use to Google and Apple data in Figure S2). Therefore, we expect the Google mobility
427 data to overestimate emission trends in the other sectors and we compare our new approach for
428 estimating granular near real time emission changes with the previous approaches of Liu et al.² and
429 Le Quéré et al.³ and with observations of NO₂ to test the assumptions.

430

431 *The Le Quéré et al. sector analysis.*

432 Le Quéré et al. analysed fossil fuel CO₂ emission changes in eight sectors (power, surface transport,
433 residential, public and commercial, industry, national shipping, international shipping, national
434 aviation and international aviation), and 69 countries representing 97% of global emissions. The Le
435 Quéré et al. estimates are based on a global estimate of sector emission reductions according to a 1-3
436 level of confinement. The confinement level estimates were obtained from government (where
437 accessible) and cross-media reports, while the sectoral activity data were from multiple streams of
438 data for each sector including industry reports, and were available daily or weekly. Changes in
439 emissions as a function of the confinement level, for each sector, were estimated by quantifying

440 changes in individual and industrial activity, in each sector as a function of the observed level of
441 confinement for all countries together. The data is then extrapolated for each country and each day
442 depending on their level of confinement and their mean emission levels in each sector. The USA and
443 China were treated at the state and provincial level, respectively. Low, medium, and high estimates of
444 the emission changes resulting from uncertainty in the activity data among countries for different
445 confinement levels were tested against our data. It was found that the high estimates agreed best with
446 the Google transit trends over Jan-Jun 2020 (see Figures 1, S1 and 2b). Projections for 2020 were also
447 provided.

448

449 *Mobility-based emission estimates.*

450 As mobility analysis does not cover all sectors or countries to make a global emission estimate we
451 combine the mobility analysis with components of the analysis in Le Quéré et al. to estimate global
452 emission changes for CO₂ and other pollutants that were due to the COVID-19 restrictions.

453 We adopt the sector approach of Le Quéré et al., but substitute their percentage changes in the
454 emissions from surface transport, residential, public and commercial and industry sectors, with
455 Google mobility changes in transit, residential, retail and recreation, and workplaces respectively. For
456 the power sector, we employed a hybrid approach, using a combined weighting of workplace,
457 residential and retail mobility weighted by the 2019 national split of industrial, residential and
458 commercial emissions. Then we used this weighted mobility measure to scale the power sector
459 emissions. Finally applying a scaling to match the global emission change in the power sector of the
460 Le Quéré et al. high estimate. We also directly employed the Le Quéré et al. emission trends for
461 international and national aviation and shipping. In the 45 countries with only Google data available,
462 the average emission changes from the 69 Le Quéré et al. nations were employed in the sectors not
463 covered by the Google mobility data. Note that for simplicity and following Le Quéré et al., shipping
464 changes are added to the surface transport trends in the analyses presented in Figure 2, S3 and S4. All
465 emission changes are compared to a daily emission rate which is the annual averaged 2019 emission
466 estimated for that country divided by 365 (using the data and approach from Le Quéré et al.). This

467 assumption was tested by analysing the Liu et al.² data which included daily seasonal variation from
468 2019 and repeating our analysis on Climate Model Intercomparison Project phase 6 (CMIP6)
469 emission data³⁴ for NO_x as a test. We found that adding a seasonal cycle would decrease the Jan -
470 May 2020 emission change estimate by 3%. However, as the Google analysis also does not account
471 for a seasonal cycle, it is difficult to gauge the overall error in our estimates. To aid comparison with
472 Le Quéré et al. and for consistency with the simple climate modelling approach discussed in methods
473 section e, we choose not to introduce a seasonal cycle in our analyses. The combined dataset gives
474 daily CO₂ emission changes for 2020, across 8 sectors and 123 countries, covering 99% of global
475 emissions. The Le Quéré et al. high estimate and new mobility-based emission estimates were found
476 to agree well with each other, both at the individual US state level and at the country level for the 56
477 countries with overlapping data (Figures S1, S3, S4 and 1b).

478 Table S1 compares the global average trends and that from some major nations to the CO₂ estimates
479 in Le Quéré et al. and that of Liu et al.². Our trends are expected to be higher than the other datasets,
480 but this doesn't manifest itself for first quarter trends in all countries. As the Google trends only start
481 on 15 February, our analysis will underestimate first quarter trend estimates where changes occurred
482 before this date. More interesting are the differences with the Liu et al.² dataset for India and Russia,
483 where their trends are considerably smaller. This could be caused by the differences with the
484 reference assumptions. The Liu et al.² approach makes a daily reference comparison with 2019
485 emissions and both nations show declining emissions in the first quarter of 2019, whereas our
486 reference is taken as the Google mobility base-period of 3 January to 6 February (see methods section
487 above). As the Le Quéré et al. emission data are well correlated in time with the Google mobility
488 estimates and also quantitatively agree (see Figure S3 and S4), we assume that the mobility trends we
489 see are largely a response to COVID-19. However, more work will be needed to fully understand and
490 resolve these differences.

491 b) Non-CO₂ emission estimates

492 The Emission Database for Global Atmospheric Research (EDGAR) version 5.0 database¹⁴ provides
493 gridded and national level sectoral emissions on methane, nitrous oxide and several short-lived
494 species. The last year available is 2015. The sectors employed in the EDGAR analyses are mapped
495 onto the Le Quéré et al. sectors used here, according to the breakdown in Table S2. The national and
496 sector level emission changes for 2020 are then estimated by equation 1.

$$\Delta E_{in,is}(t) = Ebase_{in,is} \frac{\Delta C_{in,is}(t)}{Cbase_{in,is}} \quad (1)$$

497 Where $\Delta E_{in,is}(t)$ is the emission change (in ktday⁻¹) of the species as a function of nation (*in*) and
498 sector (*is*). $Ebase_{in,is}$ is the annual emission divided by 365 of the species from the sector and nation
499 for 2015. $\Delta C_{in,is}(t)$ and $Cbase_{in,is}$ are the CO₂ emission change over 2020, and the average daily
500 baseline emission respectively in the sector and nation being considered (CO₂ is in units of MtCO₂
501 day⁻¹). Similar equations are used for international aviation and shipping, where the global emission
502 from aviation or shipping is ratioed by the globally averaged CO₂ emission change in the
503 corresponding sum over the national change in sectors from the Le Quéré et al. data. The resulting
504 changes are shown in Figures 2,3, S4 and S5. Note that only fossil fuel CO₂ emissions were accounted
505 for in Le Quéré et al., so the fractional changes refer to fossil fuel only. Agricultural and waste
506 emissions are included in non-CO₂ analyses but assumed not to change. This leads to a reduced
507 fraction of global emissions for non-CO₂ gases being covered and smaller emission changes for many
508 species (Figure 3). The assumption that a national sector's emission change will respond uniformly is
509 obviously an important one. There is limited data to explore this assumption, although Liu et al.² and
510 Le Quéré et al. discuss how well it applies for CO₂ in specific sectors in specific countries. Figures
511 ED1 and S2 and the discussion in methods section a) shows that Google mobility data is unlikely to
512 be a perfect proxy for NO_x trends in the UK but at least would be expected to be strongly correlated
513 and close to the right magnitude. This is also supported by the NO₂ analysis in Figures 3 and S7. Our
514 approach of assuming national sectors change in the same way may partly explain why timeseries for
515 CO₂ and non-CO₂ species evolve in a similar fashion in Figure 2a. However, Figure S5 shows that
516 sectors do evolve differently for different species. To examine this, we performed substitution tests

517 where we crudely made large changes to specific national sector emissions timeseries or set them to
518 zero. These tests suggested that the similar patterns seen across species in Figure 2a is more a product
519 of national restrictions evolving more-or-less together than it is of non-varying abatement choices
520 within a national sector.

521 c) Emission scenarios

522 The generated datasets above firstly combine sector specific mobility changes referenced to the 3
523 January to 6 February 2020 period, with national lockdown measures. The method then uses
524 published national emission inventories for either 2019 (for CO₂) or 2015 (for non-CO₂) to derive
525 absolute emission changes which would also be relative to the early 2020 period. This reference is
526 then projected out to 2030 to form an emission baseline representing current Nationally Determined
527 Contributions (NDCs)¹⁵. To explore the temperature response to emission changes relative to this
528 baseline, the bottom-up emission change estimates from the first four months of 2020 have been
529 extended according to the scenarios illustrated in Table 1. Four scenarios are explored: “two-year
530 blip”, “fossil-fuelled recovery”, “moderate green stimulus”, and “strong green stimulus”. The “two-
531 year blip” scenario assumes climate action to continue at the same level of ambition as implied by the
532 current NDCs¹⁵ until 2030 – approximated by the implied global carbon price consistent with the
533 emission reduction resulting from the NDCs. The “fossil-fuelled recovery” follows a path that lies
534 10% higher than the NDC path. The “moderate green stimulus” assumes about a 35% reduction in
535 total global greenhouse gas emissions relative to the baseline NDC path and a further decline of
536 global CO₂ emissions towards zero emissions in 2060. The Kyoto emissions totals of these NDC
537 baskets are broken into components using the Silicone package³⁵ by interpolating between the
538 MESSAGE-GLOBIOM implementations of the middle-of-the-road Shared Socioeconomic Pathway
539 (SSP2) scenarios^{36,37}. Where CO₂ is defined directly, we interpolate from that instead. The “strong
540 green stimulus” assumes about a 52% reduction in total global greenhouse gas emissions relative to
541 the baseline NDC path and a further decline of global CO₂ emissions towards zero emissions in 2050.
542 Non-CO₂ emissions are estimated by interpolating between the sustainability Shared Socioeconomic

543 Pathway (SSP1) scenarios implemented by the IMAGE model³⁸. Scenarios are given as emissions of
544 39 species from anthropogenic and natural sources and volcanic and solar radiative forcing (see Smith
545 et al.²² for details). Only the ten species evaluated in this paper are changed. The original dataset gives
546 annual emissions from 1750-2100, and these are linearly interpolated to monthly values, to provide
547 higher time resolution for the subsequent calculations of effective radiative forcing and temperature.

548 d) Comparison to NO₂ observations

549 Hourly observations of NO₂ are taken from the OpenAQ database (<https://openaq.org/>) between
550 January 1, 2018 and May 3, 2020, giving 1,747,189 hourly observations from 2,873 sites around the
551 world. For each observation, a spatially and temporally co-located model value for the
552 meteorological, chemical and emissions state is acquired from the NASA GEOS Composition
553 Forecast (GEOS-CF) system. GEOS-CF integrates the GEOS-Chem chemistry model into the GEOS
554 Earth System Model³⁹ providing global hourly analyses of atmospheric composition at 25x25 km²
555 spatial resolution in near real-time. Anthropogenic NO_x emissions are prescribed using monthly
556 HTAP bottom-up emissions⁴⁰, with annual scale factors based on OMI satellite data applied to it to
557 account for year-over-year changes. GEOS-CF does not account for emission reductions related to
558 COVID-19, providing a business-as-usual estimate of NO₂ that serves as a reference baseline for
559 surface observations. For each site, a function describing the time dependent model bias (observed
560 value - modelled value) is developed using the 2018 and 2019 observations based on the XGBoost
561 algorithm⁴¹, with the model meteorological, chemical and emissions state as the dependent variables.
562 50% of this data is used for training, and 50% used for testing. For 2020, we predict the concentration
563 of NO₂, by taking the model output time series of NO₂ at each station and add the bias predicted by
564 our trained algorithm. This then provides a counterfactual for the NO₂ concentration had COVID-19
565 restrictions not been put into place. We calculate the ratio between the actual concentration and that
566 predicted for each site and then take the mean across all sites within a country. These data are
567 compared to 26 country level emission estimates in Figure S7, and the country-mean reductions
568 compared to that predicted from the mobility data is shown in Figure 2b.

569 e) Surface temperature change estimates

570 From the emission scenarios in Table 1, global averaged effective radiative forcing (ERF) and near-
571 surface air temperature are computed. First, ERFs are calculated using the FaIR version 1.5 model and
572 the methodology outlined in Smith et al.²² for 13 different forcing components. Uncertainties are
573 estimated by 10,000 Monte Carlo samples of relative ERF uncertainties, using ranges based on IPCC
574 AR5⁴², see Smith et al.²² for details. NO_x emissions affect direct forcing from nitrate aerosol and
575 tropospheric ozone radiative forcing. Additionally, the ERF from aviation contrails and contrail-
576 induced cirrus is assumed to scale with NO_x emissions from the aviation sector.

577 The two layer energy balance model of Geoffroy et al.^{43,44} including efficacy of deep ocean heat
578 uptake is used to translate these ERF time series into surface temperature estimates. The five free
579 parameters in this model are chosen to match individual CMIP6 model behaviour by fitting the
580 parameters to 4xCO₂ abrupt simulations in 35 models; these parameter fits are shown in Table S3. To
581 estimate uncertainties, parameters corresponding to an individual model are picked randomly 10,000
582 times and paired to a sampled ERF parameter range for each of the 13 ERF timeseries. The two-layer
583 model is then run with each of these parameter sets to make a surface temperature projection. The
584 resulting plume of possible projections is then compared to Cowtan and Way³³ observed surface
585 temperature record. The Cowtan and Way data has been adjusted to allow for the fact the near-surface
586 air temperature has warmed more than the sea surface temperature. To make this adjustment, the
587 CMIP6 ratio of near-surface air temperature to blended near surface air temperature and surface ocean
588 temperatures is made over the historical period and found to converge towards 8% in recent years⁴⁵.
589 This is then used to scale the observations upwards. The root mean square error of the simple model
590 projections are then compared to these scaled observations over 1850-2019 inclusive. The goodness
591 of fit is then used to provide projected probability distribution based on a weighted average of the
592 goodness of fit. This follows the method outlined in Knutti et al.⁴⁶, with the exception that we do not
593 downweight ensemble members based on independence.

594 f) Testing the ozone forcing parameterisation

595 The FaIRv1.5 model used above adopts a simple global annual mean emission-forcing relationship for
596 tropospheric ozone which may not capture the seasonal and regional nuances of the atmospheric
597 chemical response to the changes in NO_x and other emissions. To test this a second ozone
598 parameterisation was employed based upon source-receptor relationships from models that
599 participated in the Task Force on Hemispheric Transport of Air Pollutants (TF-HTAP) project⁴⁷. The
600 parameterisation^{28,29} emulates the ozone response in models to applied perturbations in ozone
601 precursor emissions (NO_x, CO and NMVOCs) and global CH₄ abundance. For emission perturbations
602 in CO and NMVOCs a linear scaling factor is used whereas a non-linear factor is used for changes in
603 NO_x and CH₄. The 2020 annual mean tropospheric ozone radiative forcing and annual mean
604 tropospheric ozone burden change deduced from this parameterisation were -0.029 Wm⁻² and 7.5 Tg
605 for the high emission scenario used here.

- 606 34. Hoesly, R. *et al.* Historical (1750–2014) anthropogenic emissions of reactive gases and aerosols from
607 the Community Emissions Data System (CEDS), *Geosci. Model Dev.*, 11, 369–408 (2018).
- 608 35. Lamboll, R. D., *et al.* Silicone v1.0.0: an open-source Python package for inferring missing emissions
609 data for climate change research. *Geoscientific Model Development*. [https://doi.org/10.5194/gmd-2020-](https://doi.org/10.5194/gmd-2020-138)
610 138
- 611 36. Rogelj, J. *et al.* Scenarios towards limiting global mean temperature increase below 1.5 °C. *Nat. Clim.*
612 *Chang.* **8**, 325–332 (2018).
- 613 37. Fricko, O. *et al.* The marker quantification of the Shared Socioeconomic Pathway 2: A middle-of-the-
614 road scenario for the 21st century. *Glob. Environ. Chang.* **42**, 251–267 (2017).
- 615 38. van Vuuren, D. P. *et al.* Energy, land-use and greenhouse gas emissions trajectories under a green
616 growth paradigm. *Glob. Environ. Chang.* **42**, 237–250 (2017).
- 617 39. Hu, L. *et al.* Global simulation of tropospheric chemistry at 12.5km resolution: performance and
618 evaluation of the GEOS-Chem chemical module (v10-1) within the NASA GEOS Earth system model
619 (GEOS-5 ESM). *Geosci. Model Dev.* **11**, 4603–4620 (2018).
- 620 40. Janssens-Maenhout, G. *et al.* HTAP_v2.2: a mosaic of regional and global emission grid maps for 2008
621 and 2010 to study hemispheric transport of air pollution. *Atmos. Chem. Phys.* **15**, 11411–11432 (2015).
- 622 41. Chen, T. & Guestrin, C. XGBoost: A scalable tree boosting system. *Preprint at: arXiv:1603.02754*
623 (2016).

- 624 42. Myhre, G. et al. Anthropogenic and Natural Radiative Forcing. in *Climate Change 2013 - The Physical*
625 *Science Basis*, 659–740 (Cambridge University Press, 2013). doi:10.1017/CBO9781107415324.018
- 626 43. Geoffroy, O. et al. Transient climate response in a two-layer energy-balance model. Part I: Analytical
627 solution and parameter calibration using CMIP5 AOGCM experiments. *J. Clim.* **26**, 1841–1857 (2013).
- 628 44. Geoffroy, O. et al. Transient Climate Response in a Two-Layer Energy-Balance Model. Part II:
629 Representation of the Efficacy of Deep-Ocean Heat Uptake and Validation for CMIP5 AOGCMs. *J.*
630 *Clim.* **26**, 1859–1876 (2013).
- 631 45. Richardson, M., Cowtan, K., Hawkins, E. & Stolpe, M. B. Reconciled climate response estimates from
632 climate models and the energy budget of Earth. *Nat. Clim. Chang.* **6**, 931–935 (2016).
- 633 46. Knutti, R. et al. A climate model projection weighting scheme accounting for performance and
634 interdependence. *Geophys. Res. Lett.* **44**, 1909–1918 (2017).
- 635 47. Koffi, B. et al. Hemispheric Transport of Air Pollution (HTAP) specification of the HTAP2
636 experiments: ensuring harmonized modelling. (Publications Office of the European Union,
637 Luxembourg, 2016). doi:10.2788/725244

638

639

640 **Author contributions**

641 PMF and HIF designed the study and PMF performed the main analyses with contributions from HIF.
642 CLQ provided the original data and contributed design ideas. CJS provided the CMIP6 tuning of the
643 two layer model. CK and ME provided the surface NO₂ analyses. ST provided the ozone emulator
644 analyses. MG, C-FS contributed future scenario ideas. JR provided the scenario emission data with
645 contributions from RL. CDJ contributed the CO₂ concentration change discussion. DR contributed the
646 wider air quality and societal context discussion. TR provided the gridded online materials. All
647 authors contributed to the writing.

648

649 **Competing Interests statement**

650 The authors declare no competing interests.

651

652 **Data Availability**

653 A GitHub repository of the generated datasets and is available from [https://github.com/Priestley-](https://github.com/Priestley-Centre/COVID19_emissions)
654 [Centre/COVID19_emissions](https://github.com/Priestley-Centre/COVID19_emissions). Also on Zenodo [10.5281/zenodo.3957826](https://zenodo.org/record/105281).
655 Google LLC mobility data is available from <https://www.google.com/covid19/mobility/>
656 Apple LLC mobility data is available from <https://www.apple.com/covid19/mobility>
657 EDGAR gridded emissions data is available from
658 https://data.europa.eu/doi/10.2904/JRC_DATASET_EDGAR
659 Cowtan & Way temperature observations are available from [https://www-](https://www-users.york.ac.uk/~kdc3/papers/coverage2013/had4_krig_annual_v2_0_0.txt)
660 [users.york.ac.uk/~kdc3/papers/coverage2013/had4_krig_annual_v2_0_0.txt](https://www-users.york.ac.uk/~kdc3/papers/coverage2013/had4_krig_annual_v2_0_0.txt)
661 Le Quéré et al. (2020) emissions data are available from <https://www.icos-cp.eu/gcp-covid19>
662 The air quality data is available from <https://openaq.org/>. The GEOS modelled air pollution data used
663 in this study/project have been provided by the Global Modeling and Assimilation Office (GMAO) at
664 NASA Goddard Space Flight Center and is available from
665 <https://opendap.nccs.nasa.gov/dods/gmao/geos-cf/assim>.

666

667 Correspondence and requests for materials should be addressed to Piers Forster
668 (p.m.forster@leeds.ac.uk)

669 **Acknowledgements**

670 Funding was provided by the European Union’s Horizon 2020 Research and Innovation Programme
671 under grant agreement nos. 820829 (CONSTRAIN) and UKRI NERC grant NE/N006038/1
672 (SMURPHS). CDJ was supported by the Joint UK BEIS/Defra Met Office Hadley Centre Climate
673 Programme (GA01101) and CRESCENDO (EU Project 641816). CLQ was supported by the Royal
674 Society (grant no. RPR1\191063), and the European Commission H2020 4C grant (no. 821003). MJE
675 is grateful for computational support from the University of York’s HPC service (Viking). Stella
676 Forster is thanked for proofreading the paper and for useful ideas. Four reviewers are thanked for
677 helpful comments.

678

679

680

681 **Figure Legends**

682

683 **Figure 1.** Comparison of sector emission trends. a) Population weighted histogram of surface
684 transport trends from Apple driving data, Google transit mobility data and the high estimate from Le
685 Quéré et al. for available countries in the different datasets averaged over April 2020. b) Violin plots
686 showing the distribution, minimum, maximum and median levels of national trends weighted by CO₂
687 emissions for the Google and Le Quéré datasets and the differences between the datasets evaluated
688 over April 2020. c) Estimates of emission changes for the datasets across four sectors for April 2020
689 and the sum of the four sectors. The CO₂ emission estimates from Liu et al.² are also shown on this
690 panel. In Figures 1b and 1c data is shown for 60 countries with overlapping data in the Google and Le
691 Quéré datasets (representing 60% of global CO₂ emissions). In Figure 1c, Apple data are for 57
692 countries, covering 58% of the global emissions. The Liu et al.² estimate is for a global emission
693 change. The high estimate from Le Quéré et al. data is used in Figures 1a and 1b. Figure 1c shows the
694 Le Quéré et al. low and high estimates as the range of the error bar on the mid-level estimate. For
695 baselines, see methods section a.

696

697 **Figure 2.** Species derived changes from COVID-19 restrictions. a) Percentage globally averaged
698 emission changes for the considered species as a function of day in the year of 2020. The changes are
699 for fossil fuel CO₂ emissions and total anthropogenic emissions from the other sectors. b) A
700 breakdown of the April 2020 average global emission reductions compared to a recent year for the
701 different species. The breakdown is for major emission-nations, including international aviation.
702 Global percentage emission changes from the baseline are shown on the x-axis (see details in Figure
703 S5). Trends are relative to 2019 for CO₂, for the other species they are relative to 2015. The low, mid
704 and high estimates of the total changes based on Le Quéré et al.³ and Liu et al.² trends are shown for
705 comparison as the black circles, error bars and red triangle.

706

707 **Figure 3.** Comparison with observations. Country level comparison of the mean predicted NO_x
708 emissions change against the meteorologically-normalized observed mean fractional reduction in NO₂

709 concentration for the period 1/1/2020 to 11/5/2020. Circle size indicates the mass of NO_x emitted each
710 day for that country from EDGAR emissions. Blue line shows the line of best fit (orthogonal
711 regression) excluding China and India shown in red, weighted by the number of observations in those
712 countries, with the shaded area showing the 95% confidence interval. Not all countries are labelled.
713 Brazil shows an increase in NO₂ concentrations and is not shown but is included in the statistical fit
714 (see Figure S7).

715

716 **Figure 4.** Effective radiative forcing and temperature response. Results are for the two-year blip
717 pathway compared to the baseline pathway. The response is broken down by the major forcing
718 contributors, as emulated by the FaIRv1.5 model. 5%–95% Monte-Carlo sampled uncertainties are
719 shown and weighted according to their historical fit to the surface temperature record (see methods
720 section e).

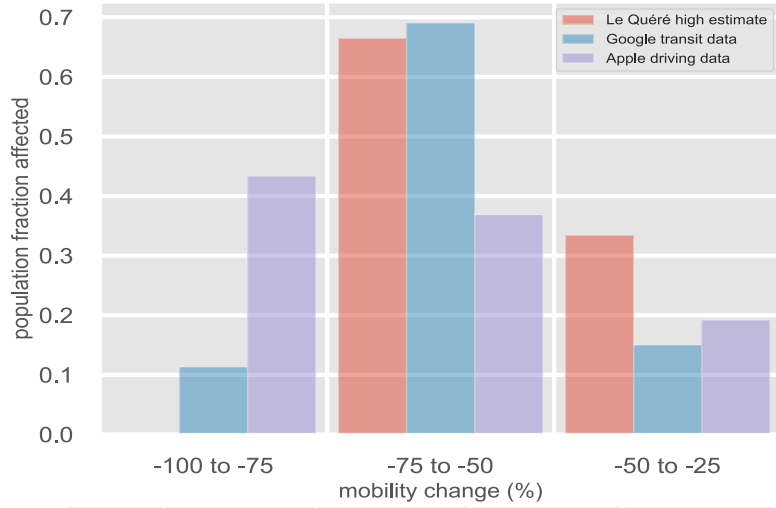
721

722 **Figure 5.** Longer term climate response. a) Emissions of CO₂, b) CO₂ concentrations, c) the surface
723 air temperature response for the what-if pathways from Table 1, emulated by the FaIRv1.5 model.
724 The baseline pathway is also plotted, but largely obscured by the two-year-blip pathway. 5%–95%
725 Monte-Carlo sampled uncertainties are shown and weighted according to their historical fit to
726 observations³³ shown in panel c (see methods section e).

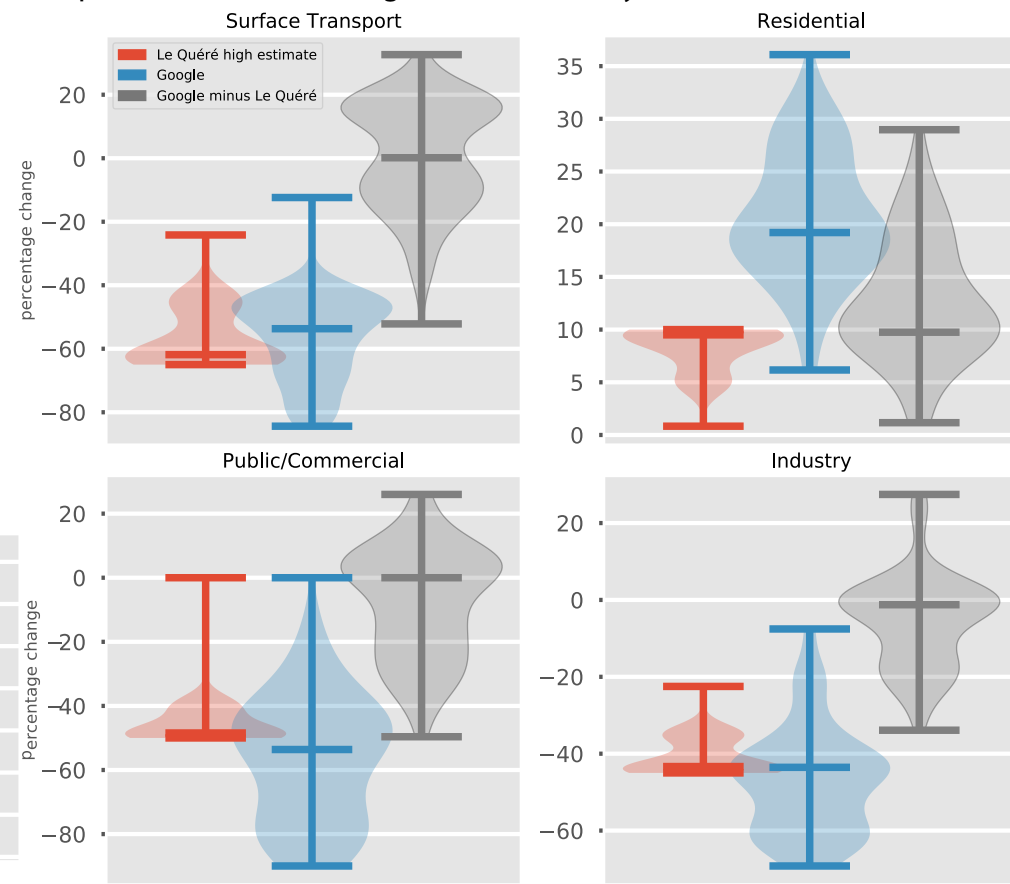
727

a) April 2020 changes in mobility

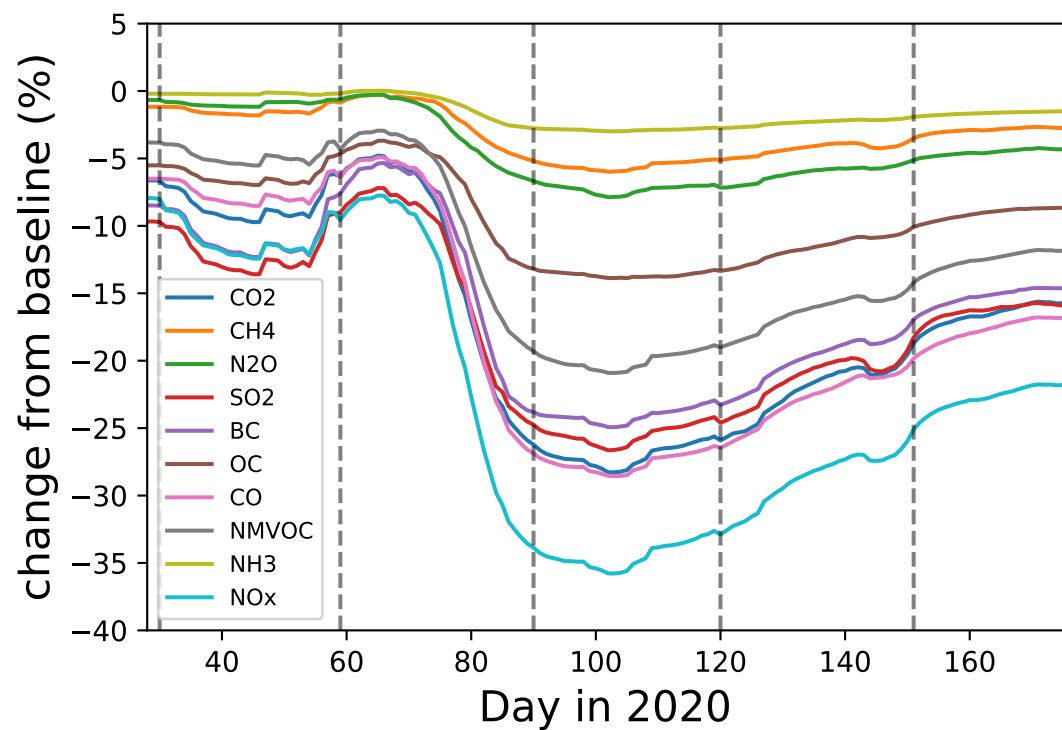
a) April 2020 changes in mobility



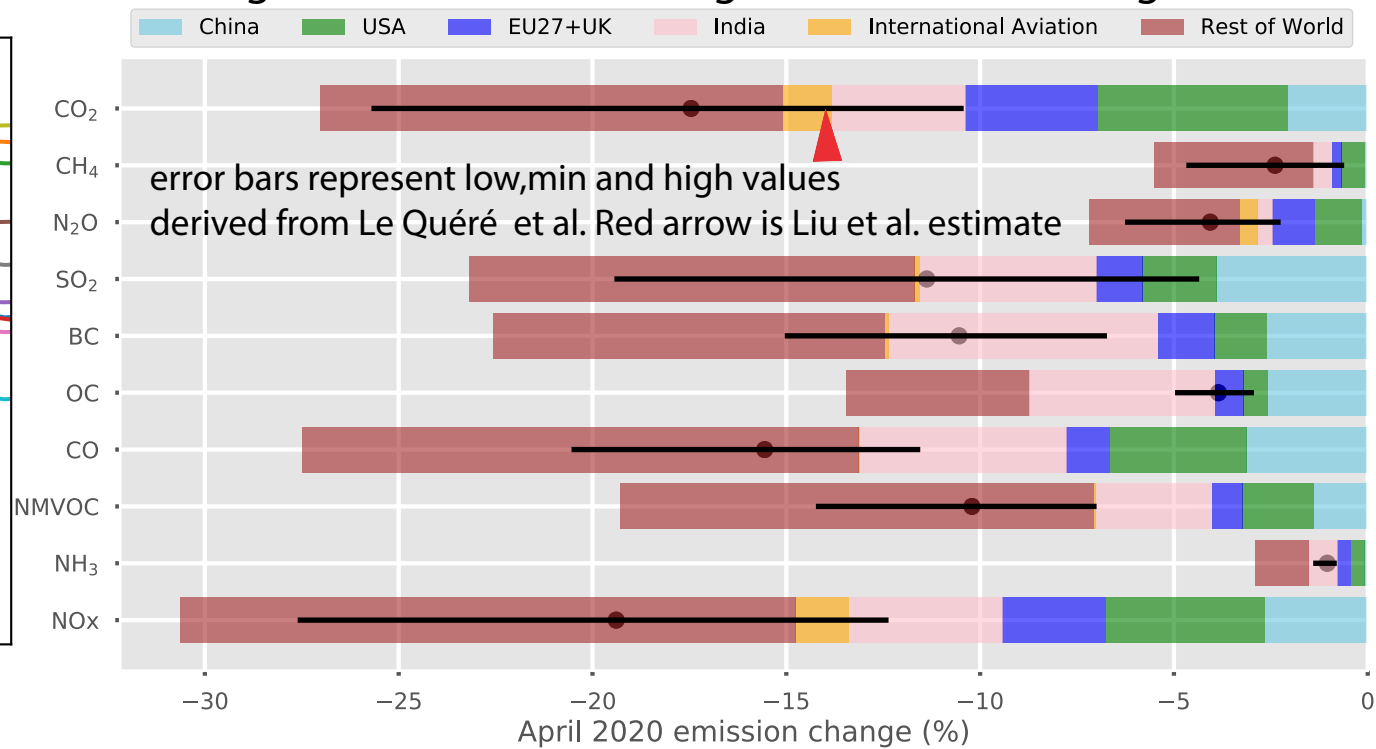
b) April 2020 national changes in emissions by sectors

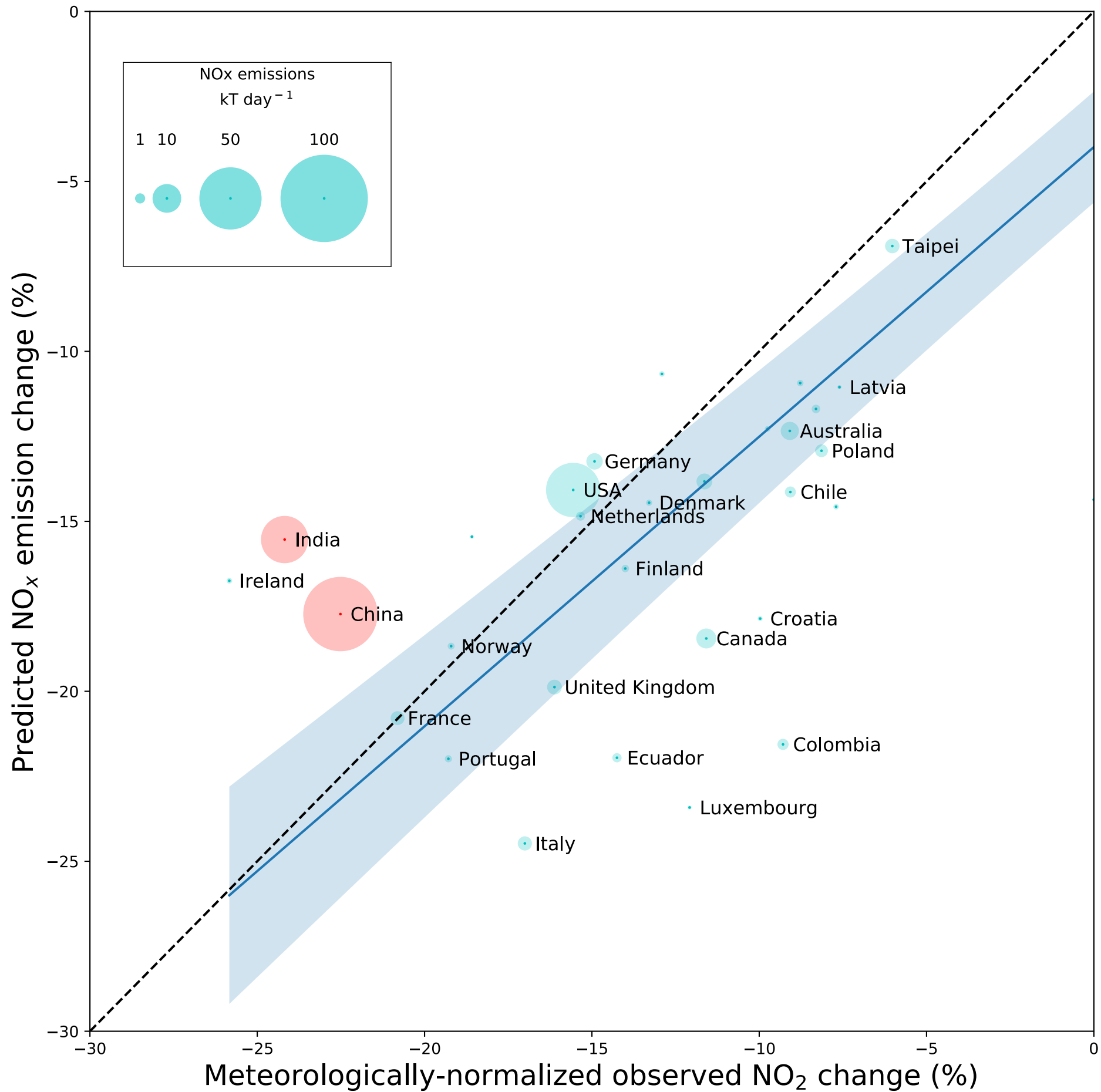


a) Febuary - June 2020 emission change by species

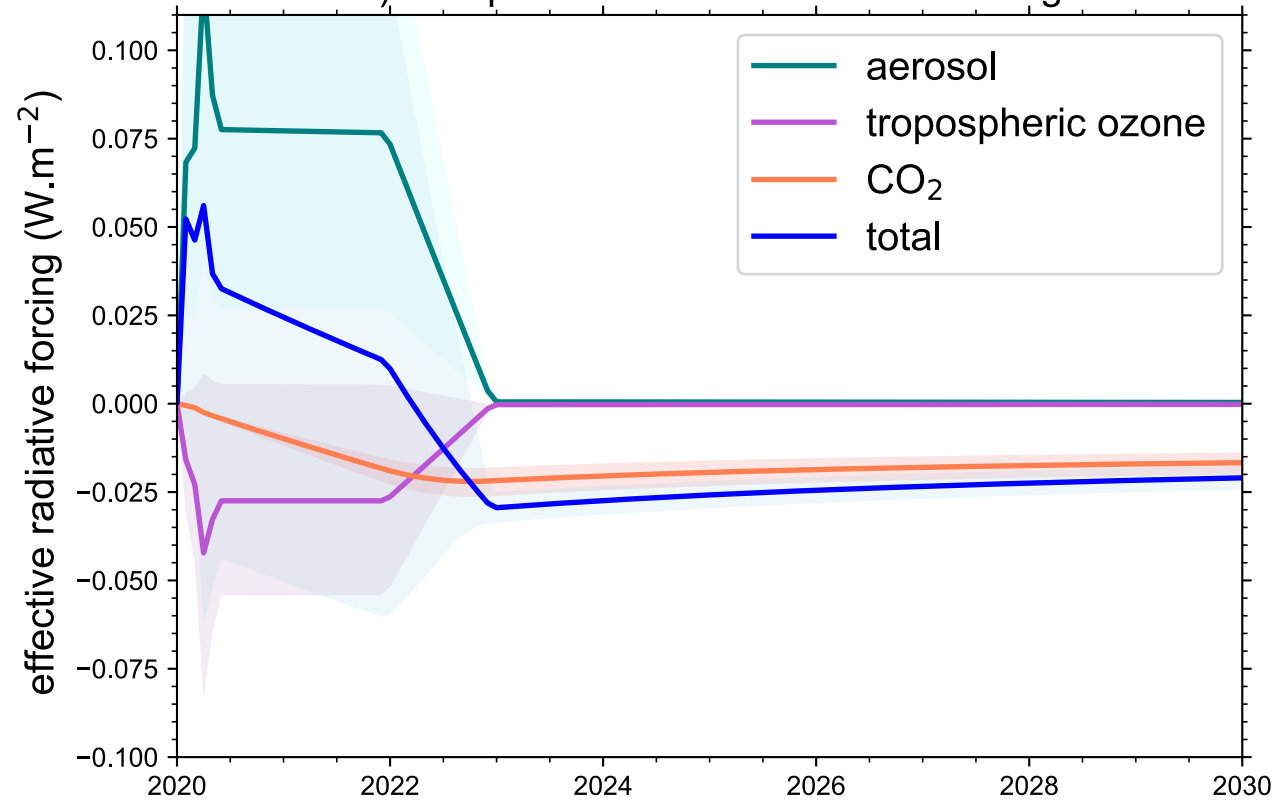


b) regional contributions to global emission change

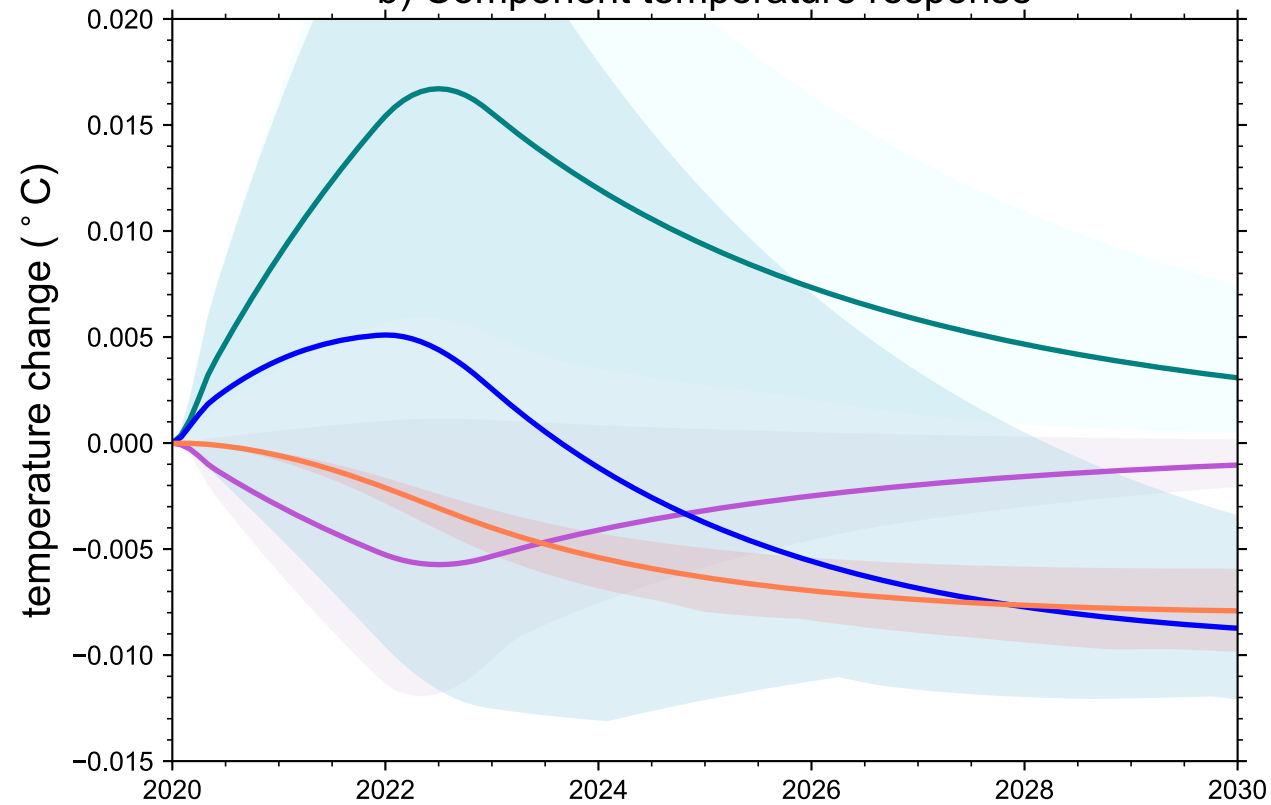


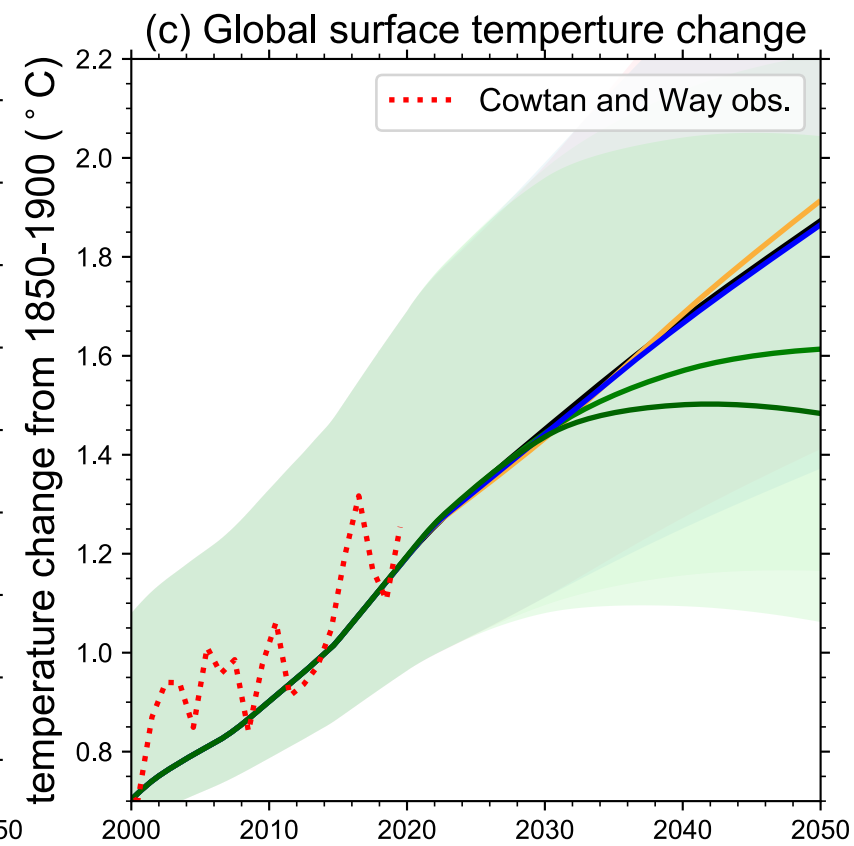
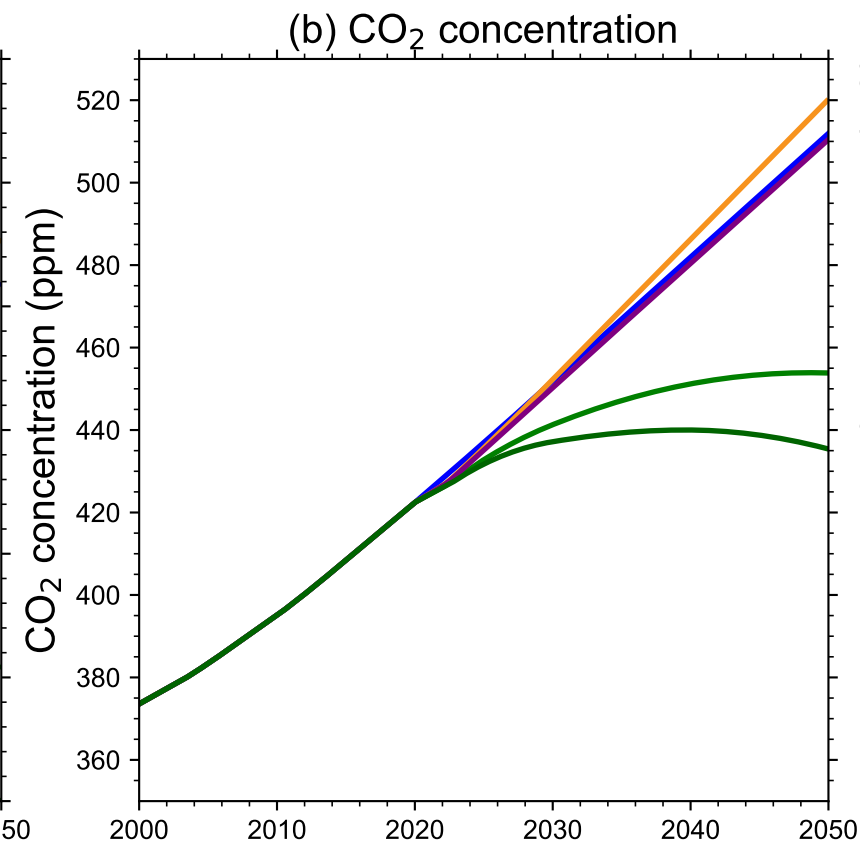
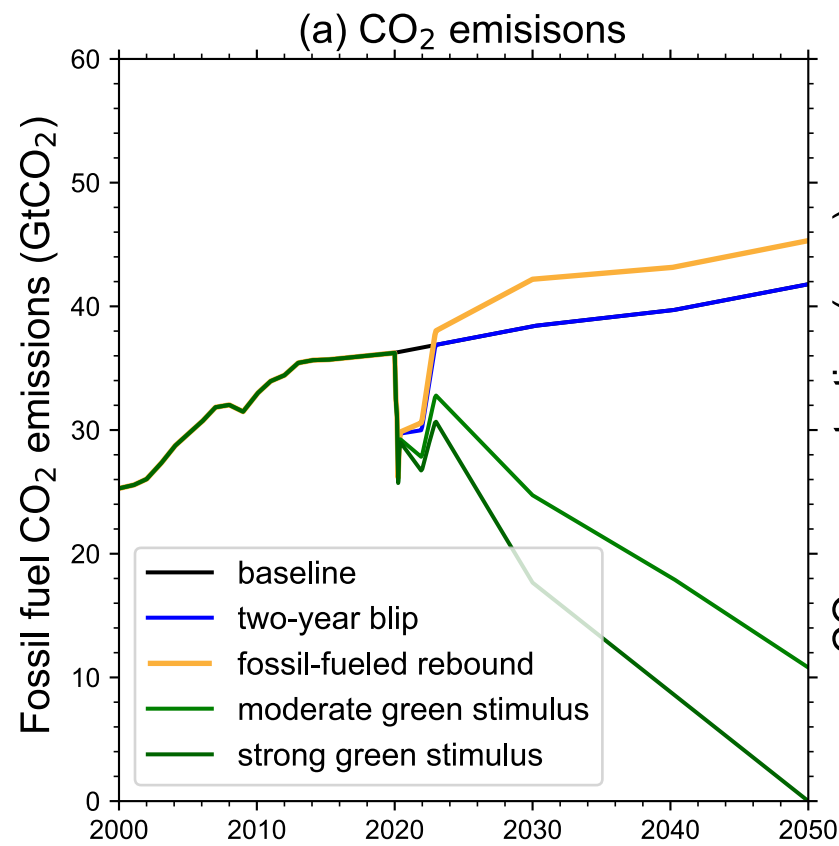


a) Component effective radiative forcing



b) Component temperature response





1
2
3

1. Extended Data

Figure #	Figure title One sentence only	Filename This should be the name the file is saved as when it is uploaded to our system. Please include the file extension. i.e.: <i>Smith_ED_Fi_1.jpg</i>	Figure Legend If you are citing a reference for the first time in these legends, please include all new references in the Online Methods References section, and carry on the numbering from the main References section of the paper.
Extended Data Fig. 1	Comparison of Google and Apple data	FigED1.eps	Comparison of Google and Apple data. The Apple driving change in April plotted against the Google transit change for available nations. Example countries are highlighted. The size of the symbol gives a measure of the correlation over Feb-June 2020, ranging from 0.39 for Sweden to over 0.96 (India). The dashed line indicates equality.
Extended Data Fig. 2	Two-year blip scenario	FigED2.eps	Two-year blip scenario. Emissions, and best estimates of CO ₂ concentration and effective radiative forcing (ERFs) components from the two-year blip scenario. Component ERFs are shown with minor ERFs in panel b) and the three largest ERF changes in c).
Extended Data Fig. 3	Longer term climate projections to 2030	FigED3.eps	Longer term climate projections to 2030. Emissions, ERF and temperature response from the three scenarios over 2019-2030 (top). The probabilities are generated by varying the emulated CMIP6 model (one of 35) and ERF ranges with a 10,000 Monte Carlo sample. Distributions are weighted according to their goodness of fit over the historical period (see methods section e).
Extended Data Fig. 4	Longer term climate projections to 2050	FigED4.eps	Longer term climate projections to 2050. As Figure ED3 except for the period extended to 2019-2050.

Extended Data Fig. 5	Probability distributions of passing 2050 global warming levels	FigED5.eps	Probability distributions of passing 2050 global warming levels. Levels are relative to 1850-1900 for the scenarios in Table 1, generated by varying the emulated CMIP6 model (choosing one of 35 model formulations) and ERF ranges. Distributions are weighted according to their goodness of fit over the historical period (see methods section e).
----------------------	---	------------	---

4 **2. Supplementary Information:**

5 **A. Flat Files**

Item	Present?	Filename This should be the name the file is saved as when it is uploaded to our system, and should include the file extension. The extension must be .pdf	A brief, numerical description of file contents. i.e.: <i>Supplementary Figures 1-4, Supplementary Discussion, and Supplementary Tables 1-4.</i>
Supplementary Information	Yes	Covid_emissions_paperV3_clean_supplementary.pdf	<i>Supplementary Figures 1-7 and Supplementary Tables 1-4</i>
Reporting Summary	No		

6
7

8 **B. Additional Supplementary Files**

Type	Number If there are multiple files of the same type this should be the numerical indicator. i.e. "1" for Video 1, "2" for Video 2, etc.	Filename This should be the name the file is saved as when it is uploaded to our system, and should include the file extension. i.e.: <i>Smith_Supplementary_Video_1.mov</i>	Legend or Descriptive Caption Describe the contents of the file
Choose an item.			

9

10 **3. Source Data**

Parent Figure or Table	Filename This should be the name the file is saved as when it is uploaded to our system, and should include the file extension. i.e.: <i>Smith_SourceData_Fig1.xls</i> , or <i>Smith_Unmodified_Gels_Fig1.pdf</i>	Data description e.g.: Unprocessed Western Blots and/or gels, Statistical Source Data, etc.
Source Data Fig. 1		